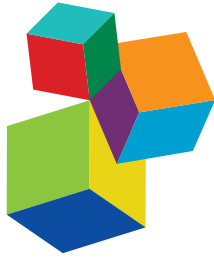


# ACIDIFICATION AND HYPOXIA IN MARGINAL SEAS

EDITED BY: Xianghui Guo, Hongjie Wang, Richard Alan Feely,  
Arnaud Laurent and Nina Bednarsek

PUBLISHED IN: *Frontiers in Marine Science*



# frontiers

## Frontiers eBook Copyright Statement

The copyright in the text of individual articles in this eBook is the property of their respective authors or their respective institutions or funders. The copyright in graphics and images within each article may be subject to copyright of other parties. In both cases this is subject to a license granted to Frontiers.

The compilation of articles constituting this eBook is the property of Frontiers.

Each article within this eBook, and the eBook itself, are published under the most recent version of the Creative Commons CC-BY licence.

The version current at the date of publication of this eBook is CC-BY 4.0. If the CC-BY licence is updated, the licence granted by Frontiers is automatically updated to the new version.

When exercising any right under the CC-BY licence, Frontiers must be attributed as the original publisher of the article or eBook, as applicable.

Authors have the responsibility of ensuring that any graphics or other materials which are the property of others may be included in the CC-BY licence, but this should be checked before relying on the CC-BY licence to reproduce those materials. Any copyright notices relating to those materials must be complied with.

Copyright and source acknowledgement notices may not be removed and must be displayed in any copy, derivative work or partial copy which includes the elements in question.

All copyright, and all rights therein, are protected by national and international copyright laws. The above represents a summary only. For further information please read Frontiers' Conditions for Website Use and Copyright Statement, and the applicable CC-BY licence.

ISSN 1664-8714  
ISBN 978-2-88976-253-8  
DOI 10.3389/978-2-88976-253-8

## About Frontiers

Frontiers is more than just an open-access publisher of scholarly articles: it is a pioneering approach to the world of academia, radically improving the way scholarly research is managed. The grand vision of Frontiers is a world where all people have an equal opportunity to seek, share and generate knowledge. Frontiers provides immediate and permanent online open access to all its publications, but this alone is not enough to realize our grand goals.

## Frontiers Journal Series

The Frontiers Journal Series is a multi-tier and interdisciplinary set of open-access, online journals, promising a paradigm shift from the current review, selection and dissemination processes in academic publishing. All Frontiers journals are driven by researchers for researchers; therefore, they constitute a service to the scholarly community. At the same time, the Frontiers Journal Series operates on a revolutionary invention, the tiered publishing system, initially addressing specific communities of scholars, and gradually climbing up to broader public understanding, thus serving the interests of the lay society, too.

## Dedication to Quality

Each Frontiers article is a landmark of the highest quality, thanks to genuinely collaborative interactions between authors and review editors, who include some of the world's best academicians. Research must be certified by peers before entering a stream of knowledge that may eventually reach the public - and shape society; therefore, Frontiers only applies the most rigorous and unbiased reviews. Frontiers revolutionizes research publishing by freely delivering the most outstanding research, evaluated with no bias from both the academic and social point of view. By applying the most advanced information technologies, Frontiers is catapulting scholarly publishing into a new generation.

## What are Frontiers Research Topics?

Frontiers Research Topics are very popular trademarks of the Frontiers Journals Series: they are collections of at least ten articles, all centered on a particular subject. With their unique mix of varied contributions from Original Research to Review Articles, Frontiers Research Topics unify the most influential researchers, the latest key findings and historical advances in a hot research area! Find out more on how to host your own Frontiers Research Topic or contribute to one as an author by contacting the Frontiers Editorial Office: [frontiersin.org/about/contact](https://frontiersin.org/about/contact)

# ACIDIFICATION AND HYPOXIA IN MARGINAL SEAS

Topic Editors:

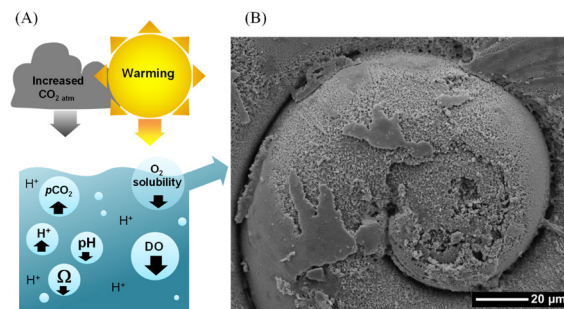
**Xianghui Guo**, Xiamen University, China

**Hongjie Wang**, University of Rhode Island, United States

**Richard Alan Feely**, Pacific Marine Environmental Laboratory, National Oceanic and Atmospheric Administration (NOAA), United States

**Arnaud Laurent**, Dalhousie University, Canada

**Nina Bednarsek**, National Institute of Biology (NIB), Slovenia



The image is modified based on Figure 1a of Lucey *et al.* (this Research Topic) and Figure 7b of Niemi *et al.* (this Research Topic). (A) Graphical depiction of atmospheric warming and increasing atmospheric carbon dioxide ( $\text{CO}_{2\text{atm}}$ ), which drives ocean warming, contribute to the decreases in dissolved oxygen (DO), and lowers pH and saturation state index of calcium carbonate ( $\Omega$ ). The partial pressure of  $\text{CO}_2$  ( $p\text{CO}_2$ ) increases due to increasing atmospheric  $\text{CO}_2$  that is absorbed into the seawater (i.e., ocean acidification), along with other biological processes in the marine environment. (B) Scanning Electron Microscope (SEM) image showing dissolution on pteropod shells collected in the Amundsen Gulf in the Canadian Arctic, in 2017.

Lucey N, Haskett E and Collin R (2020) Multi-stressor Extremes Found on a Tropical Coral Reef Impair Performance. *Front. Mar. Sci.* 7:588764. doi: 10.3389/fmars.2020.588764

Niemi A, Bednaršek N, Michel C, Feely RA, Williams W, Azetsu-Scott K, Walkusz W and Reist JD (2021) Biological Impact of Ocean Acidification in the Canadian Arctic: Widespread Severe Pteropod Shell Dissolution in Amundsen Gulf. *Front. Mar. Sci.* 8:600184. doi: 10.3389/fmars.2021.600184

**Citation:** Guo, X., Wang, H., Feely, R. A., Laurent, A., Bednarsek, N., eds. (2022). *Acidification and Hypoxia in Marginal Seas*. Lausanne: Frontiers Media SA. doi: 10.3389/978-2-88976-253-8

# Table of Contents

## **07 Editorial: Acidification and Hypoxia in Marginal Seas**

Xianghui Guo, Nina Bednaršek, Hongjie Wang, Richard A. Feely and Arnaud Laurent

## **CHAPTER 1**

### **OCEAN ACIDIFICATION AND DEOXYGENATION IN MARGINAL SEAS RIVER DOMINATED MARGINS**

#### **12 Comparing Subsurface Seasonal Deoxygenation and Acidification in the Yellow Sea and Northern East China Sea Along the North-to-South Latitude Gradient**

Tian-qi Xiong, Qin-sheng Wei, Wei-dong Zhai, Cheng-long Li, Song-yin Wang, Yi-xing Zhang, Shuo-jiang Liu and Si-qing Yu

#### **33 Clarifying Water Column Respiration and Sedimentary Oxygen Respiration Under Oxygen Depletion Off the Changjiang Estuary and Adjacent East China Sea**

Jun Zhou, Zhuo-Yi Zhu, Huan-Ting Hu, Gui-Ling Zhang and Qian-Qian Wang

#### **49 Intrusion of Kuroshio Helps to Diminish Coastal Hypoxia in the Coast of Northern South China Sea**

Hon-Kit Lui, Chen-Tung Arthur Chen, Wei-Ping Hou, Jian-Ming Liao, Wen-Chen Chou, You-Lin Wang, Chau-Ron Wu, Jay Lee, Yi-Chia Hsin and Yan-Yu Choi

#### **62 Advances on Coastal and Estuarine Circulations Around the Changjiang Estuary in the Recent Decades (2000–2020)**

Zhiqiang Liu, Jianping Gan, Hui Wu, Jianyu Hu, Zhongya Cai and Yongfei Deng

#### **81 Temporal and Spatial Variability of the CO<sub>2</sub> System in a Riverine Influenced Area of the Mediterranean Sea, the Northern Adriatic**

Lidia Urbini, Gianmarco Inghrosso, Tamara Djakovac, Salvatore Piacentino and Michele Giani

#### **102 Effects of Wind-Driven Lateral Upwelling on Estuarine Carbonate Chemistry**

Ming Li, Renjian Li, Wei-Jun Cai, Jeremy M. Testa and Chunqi Shen

#### **121 Inter-annual Variability of the Carbonate System in the Hypoxic Upper Pearl River Estuary in Winter**

Xianghui Guo, Xue Song, Ying Gao, Yaohua Luo, Yi Xu, Tao Huang and Lifang Wang

#### **136 Seasonal Mixing and Biological Controls of the Carbonate System in a River-Dominated Continental Shelf Subject to Eutrophication and Hypoxia in the Northern Gulf of Mexico**

Wei-Jen Huang, Wei-Jun Cai and Xinping Hu

## NON-RIVER DOMINATED MARGINS

- 155** *Summertime Oxygen Depletion and Acidification in Bohai Sea, China*  
Guisheng Song, Liang Zhao, Fei Chai, Fangfang Liu, Mengting Li and Huixiang Xie
- 166** *Ocean Acidification State in the Highly Eutrophic Tokyo Bay, Japan: Controls on Seasonal and Interannual Variability*  
Michiyo Yamamoto-Kawai, Soichiro Ito, Haruko Kurihara and Jota Kanda
- 179** *Continuous Monitoring and Future Projection of Ocean Warming, Acidification, and Deoxygenation on the Subarctic Coast of Hokkaido, Japan*  
Masahiko Fujii, Shintaro Takao, Takuto Yamaka, Tomoo Akamatsu, Yamato Fujita, Masahide Wakita, Akitomo Yamamoto and Tsuneo Ono
- 191** *High-Resolution Carbonate System Dynamics of Netarts Bay, OR From 2014 to 2019*  
William Fairchild and Burke Hales
- 207** *The Mid-Atlantic Bight Dissolved Inorganic Carbon System Observed in the March 1996 DOE Ocean Margins Program (OMP)—A Baseline Study*  
Ting-Hsuan Huang, Wei-Jun Cai, Penny Vlahos, Douglas W. R. Wallace, Ernie R. Lewis and Chen-Tung Arthur Chen
- 223** *Ecosystem Metabolism Modulates the Dynamics of Hypoxia and Acidification Across Temperate Coastal Habitat Types*  
Ryan B. Wallace, Bradley J. Peterson and Christopher J. Gobler

## CHAPTER 2

### OCEAN ACIDIFICATION AND HYPOXIA AT THE CHEMICAL-BIOLOGICAL INTERFACE

- 243** *Early Diagenesis in the Hypoxic and Acidified Zone of the Northern Gulf of Mexico: Is Organic Matter Recycling in Sediments Disconnected From the Water Column?*  
Christophe Rabouille, Bruno Lansard, Shannon M. Owings, Nancy N. Rabalais, Bruno Bombled, Edouard Metzger, Julien Richirt, Eryn M. Eitel, Anthony D. Boever, Jordon S. Beckler and Martial Taillefert
- 261** *Massive Methane Loss During Seasonal Hypoxia/Anoxia in the Nearshore Waters of Southeastern Arabian Sea*  
V. Sudheesh, G. V. M. Gupta and S. W. A. Naqvi
- 274** *Massive Nitrogen Loss Over the Western Indian Continental Shelf During Seasonal Anoxia: Evidence From Isotope Pairing Technique*  
Amit Sarkar, Syed Wajih Ahmad Naqvi, Gaute Lavik, Anil Pratihary, Hema Naik, Gayatri Shirodkar and Marcel M. M. Kuypers
- 288** *Early Diagenesis in Sediments of the Venice Lagoon (Italy) and Its Relationship to Hypoxia*  
Daniele Brigolin, Christophe Rabouille, Clément Demasy, Bruno Bombled, Gaël Monvoisin and Roberto Pastres

## CHAPTER 3

### IMPACTS OF OCEAN ACIDIFICATION AND HYPOXIA ON MARINE ORGANISMS AND ECOSYSTEMS

- 303** *Interactive Effects of Elevated CO<sub>2</sub> Concentration and Light on the Picophytoplankton Synechococcus*  
Nanou Bao and Kunshan Gao
- 310** *Response of Phytoplankton Assemblages From Naturally Acidic Coastal Ecosystems to Elevated pCO<sub>2</sub>*  
Natalia Osma, Laura Latorre-Melín, Bárbara Jacob, Paulina Y. Contreras, Peter von Dassow and Cristian A. Vargas
- 331** *Elevated pCO<sub>2</sub> Impedes Succession of Phytoplankton Community From Diatoms to Dinoflagellates Along With Increased Abundance of Viruses and Bacteria*  
Ruiping Huang, Jiazhen Sun, Yunlan Yang, Xiaowen Jiang, Zhen Wang, Xue Song, Tifeng Wang, Di Zhang, He Li, Xiangqi Yi, Shouchang Chen, Nanou Bao, Liming Qu, Rui Zhang, Nianzhi Jiao, Yahui Gao, Bangqin Huang, Xin Lin, Guang Gao and Kunshan Gao
- 345** *The Combined Effects of Increased pCO<sub>2</sub> and Warming on a Coastal Phytoplankton Assemblage: From Species Composition to Sinking Rate*  
Yuanyuan Feng, Fei Chai, Mark L. Wells, Yan Liao, Pengfei Li, Ting Cai, Ting Zhao, Feixue Fu and David A. Hutchins
- 360** *Multi-stressor Extremes Found on a Tropical Coral Reef Impair Performance*  
Noelle Lucey, Eileen Haskett and Rachel Collin
- 374** *Marine Heatwaves, Sewage and Eutrophication Combine to Trigger Deoxygenation and Biodiversity Loss: A SW Atlantic Case Study*  
Kalina M. Brauko, Alex Cabral, Natasha V. Costa, Juliana Hayden, Carlos E. P. Dias, Edilene S. Leite, Renan D. Westphal, Carolina M. Mueller, Jason M. Hall-Spencer, Regina R. Rodrigues, Leonardo R. Rörig, Paulo R. Pagliosa, Alessandra L. Fonseca, Orestes E. Alarcon and Paulo A. Horta
- 385** *Ocean Acidification Amplifies Multi-Stressor Impacts on Global Marine Invertebrate Fisheries*  
Travis C. Tai, U. Rashid Sumaila and William W. L. Cheung
- 397** *Synthesis of Thresholds of Ocean Acidification Impacts on Echinoderms*  
Nina Bednaršek, Piero Calosi, Richard A. Feely, Richard Ambrose, Maria Byrne, Kit Yu Karen Chan, Sam Dupont, Jacqueline L. Padilla-Gamiño, John I. Spicer, Faycal Kessouri, Miranda Roethler, Martha Sutula and Stephen B. Weisberg
- 412** *Molecular Biomarkers of the Mitochondrial Quality Control are Differently Affected by Hypoxia-Reoxygenation Stress in Marine Bivalves Crassostrea gigas and Mytilus edulis*  
Jennifer B. M. Steffen, Halina I. Falfushynska, Helen Piontkivska and Inna M. Sokolova
- 431** *Biological Impact of Ocean Acidification in the Canadian Arctic: Widespread Severe Pteropod Shell Dissolution in Amundsen Gulf*  
Andrea Niemi, Nina Bednaršek, Christine Michel, Richard A. Feely, William Williams, Kumiko Azetsu-Scott, Wojciech Walkusz and James D. Reist

**447 *Comparative Sensitivities of Zooplankton to Ocean Acidification Conditions in Experimental and Natural Settings***

Katherine E. Keil, Terrie Klinger, Julie E. Keister and Anna K. McLaskey

**455 *Integrated Assessment of Ocean Acidification Risks to Pteropods in the Northern High Latitudes: Regional Comparison of Exposure, Sensitivity and Adaptive Capacity***

Nina Bednaršek, Kerry-Ann Naish, Richard A. Feely, Claudine Hauri, Katsunori Kimoto, Albert J. Hermann, Christine Michel, Andrea Niemi and Darren Pilcher

**478 *Distribution and Activity of Ammonia-Oxidizers on the Size-Fractionated Particles in the Pearl River Estuary***

Li Ma, Shangjin Tan, Hongbin Liu, Shuh-Ji Kao, Minhan Dai and Jin-Yu Terence Yang

## **CHAPTER 4**

### **LONG-TERM VARIABILITY IN OCEAN ACIDIFICATION AND HYPOXIA IN MARGINAL SEAS**

**489 *Deoxygenation in Marginal Seas of the Indian Ocean***

S. Wajih A. Naqvi

**505 *Decadal Dynamics of the CO<sub>2</sub> System and Associated Ocean Acidification in Coastal Ecosystems of the North East Atlantic Ocean***

Jean-Philippe Gac, Pierre Marrec, Thierry Cariou, Emilie Grosstefan, Éric Macé, Peggy Rimmelin-Maury, Marc Vernet and Yann Bozec

**531 *Climate and Human-Driven Variability of Summer Hypoxia on a Large River-Dominated Shelf as Revealed by a Hypoxia Index***

Kui Wang, Wei-Jun Cai, Jianfang Chen, David Kirchman, Bin Wang, Wei Fan and Daji Huang



# Editorial: Acidification and Hypoxia in Marginal Seas

Xianghui Guo<sup>1\*</sup>, Nina Bednaršek<sup>2</sup>, Hongjie Wang<sup>3</sup>, Richard A. Feely<sup>4</sup> and Arnaud Laurent<sup>5</sup>

<sup>1</sup> State Key Laboratory of Marine Environmental Science, College of Ocean and Earth Sciences, Xiamen University, Xiamen, China, <sup>2</sup> National Institute of Biology, Marine Biology Station Piran, Piran, Slovenia, <sup>3</sup> Graduate School of Oceanography, University of Rhode Island, Narragansett, RI, United States, <sup>4</sup> National Oceanic and Atmospheric Administration (NOAA) Pacific Marine Environmental Laboratory, Seattle, WA, United States, <sup>5</sup> Department of Oceanography, Dalhousie University, Halifax, NS, Canada

**Keywords:** ocean acidification, hypoxia, marginal seas, biological impacts, long-term variation

## Editorial on the Research Topic

### Acidification and Hypoxia in Marginal Seas

## ACIDIFICATION AND DEOXYGENATION IN MARGINAL SEAS

Ocean acidification and hypoxia (dissolved oxygen  $<2 \text{ mg L}^{-1}$  or  $<62 \mu\text{mol L}^{-1}$ ) are universal environmental concerns that can impact ecological and biogeochemical processes, including element cycling, carbon sequestration, community shifts, contributing to biodiversity reduction, and reducing marine ecosystem services (Riebesell et al., 2000; Feely et al., 2004, 2009; Andersson et al., 2005; Doney, 2006; Cohen and Holcomb, 2009; Doney et al., 2009, 2020; Kleypas and Yates, 2009; Ekstrom et al., 2015; Gattuso et al., 2015). While the stressors are global in their occurrence, local and regional impacts might be enhanced and even more accelerated, thus requiring even greater and faster consideration (Doney et al., 2020).

The driving mechanisms of acidification and hypoxia are inextricably linked in near-shore and coastal habitats. Along coastal shelf and its adjacent marginal seas, where the natural variability of multiple stressors is high, human-induced eutrophication is additionally enhancing both local acidification and hypoxia. For example, the well-known eutrophication of surface waters in the northern Gulf of Mexico caused hypoxic conditions that result in a pH decrease by 0.34 in the oxygen-depleted bottom water, which is significantly more than the pH decrease via atmospheric CO<sub>2</sub> sequestration alone (pH decrease by 0.11; Cai et al., 2011). Similar changes in coastal conditions involving biological respiration and atmospheric CO<sub>2</sub> invasion have also been observed in other marginal seas, urbanized estuaries, salt marshes and mangroves (Feely et al., 2008, 2010, 2018; Cai et al., 2011; Howarth et al., 2011). Other natural and anthropogenic processes, such as increased wind intensity and coastal upwelling, enhanced stratification due to global warming, along with more intense benthic respiration, more frequent extreme events, oscillation of water circulations, and variations in the terrestrial carbon and/or alkalinity fluxes, etc., all influence the onset and maintenance of acidification and/or hypoxia. For example, coastal upwelling brings both low pH and hypoxic water from below and enhances acidification and hypoxia in the coastal regions (Feely et al., 2008). Although acidification and hypoxia in the open oceans have received considerable attention already, the advances in our understanding of the driving mechanisms and the temporal evolution under global climate change is still poorly understood, particularly with respect to the region-specific differences, various scales of temporal and spatial variability, predictability patterns, and interactive multiple stressor impacts. Therefore, coastal ecosystems have a much broader range of rates of change in pH than the open ocean does (Carstensen and Duarte, 2019). The importance of understanding acidification and hypoxia for the biogeochemical and ecosystem implications in marginal seas is essential for climate change mitigation and adaptation strategy implementations in the future.

## OPEN ACCESS

### Edited and reviewed by:

Marta Marcos,  
University of the Balearic  
Islands, Spain

### \*Correspondence:

Xianghui Guo  
xhguo@xmu.edu.cn

### Specialty section:

This article was submitted to  
Coastal Ocean Processes,  
a section of the journal  
Frontiers in Marine Science

**Received:** 25 January 2022

**Accepted:** 25 February 2022

**Published:** 31 March 2022

### Citation:

Guo X, Bednaršek N, Wang H,  
Feely RA and Laurent A (2022)  
Editorial: Acidification and Hypoxia in  
Marginal Seas.  
Front. Mar. Sci. 9:861850.  
doi: 10.3389/fmars.2022.861850

The scope of this Research Topic is to cover the most recent advances related to the status of acidification and hypoxia in marginal seas, the coupling mechanisms of multi-drivers and human impacts, ecosystem responses, prediction of their evolution over space and time, and under future climate change scenarios. The authors of this Research Topic contributed a total of 35 papers covering a wide variety of subjects spanning from acidification and/or hypoxia (OAH) status, the carbonate chemistry baseline and trends, the impacts of OAH on the habitat suitability and ecosystem implications, and the long-term changes and variability of OAH in marginal seas.

Across many different temporal and spatial scales, the contributed papers highlighted the presence of acidification and hypoxia with their major controls in the marginal seas of the North Pacific, including the subpolar Bering Sea, the temperate China Seas of Bohai Sea, Yellow Sea and the East China Sea, Japanese coasts (Tokyo Bay and the coast of Hokkaido); the Atlantic, including the northern Gulf of Mexico, the Chesapeake Bay, and the Mediterranean Sea; the Arctic, including the Amundsen Gulf; the Indian Ocean, including the Arabian Sea, the Red Sea, etc.

In the large river dominated East China Sea shelf, hypoxia occurs in bottom waters in summer (Li et al., 2002; Zhu et al., 2017). Circulation plays an important role in the biogeochemical processes including redistribution of nutrients, changes in stratification, water residence time and ventilation of the shelf water (Liu et al.). Furthermore, the impact of typhoons results in hypoxia demise with immediate extensive vertical mixing. However, the excess freshwater and nutrient loading during the typhoon period would boost the hypoxia restoration later on when the shelf waters are re-stratified (Liu et al.). With respect to coastal oxygen consumption, water, and sediment interactions contribute dynamically, and water-column respiration processes contribute to as much as 24–69% of total oxygen consumption beneath the pycnocline (Zhou et al.). Deconvolving the water column vs. sedimentary oxygen respiration in the oxygen depletion off the Changjiang estuary and East China Sea is an important advancement of our understanding of oxygen sinks.

From the perspective of a comparison between the northern East China Sea and the adjacent southern Yellow Sea, higher CO<sub>2</sub> solubility together with the biogeochemical CO<sub>2</sub> additions caused the colder Yellow Sea water generally to have lower aragonite saturation state index ( $\Omega_{Ar}$ ) than the warmer northern East China Sea water (Xiong et al.). Although marine organic matter is the major source of the oxygen-consuming carbon in the large river-dominated margins (Green et al., 2006; Wang et al., 2016), the maximum of hypoxia may come at a significant lag from the time of peak productivity. For example, bottom water hypoxia and acidification has a 2-month delay when compared with the maximum primary production in surface waters of the northern Gulf of Mexico (Huang W-J. et al.).

In addition to biogeochemical processes, upwelling also plays an important role in the status and distribution of hypoxia/acidification occurrence, such as in the well-known upwelling region off the California coast (Feely et al., 2008, 2016). The Chesapeake Bay is also impacted by upwelling-induced acidification, which will intensify with the wind-driven upwelling to cause low pH and “corrosive” water in the shallow shoals of

the estuaries, enhancing large temporal pH and  $\Omega_{Ar}$  seasonal fluctuations (Li et al.). Furthermore, non-local mechanisms may also be important in regulating the occurrence of hypoxia. For example, the Kuroshio intrusion into the northern South China Sea relieves the occurrence of hypoxia in the coastal zone (Lui et al.).

In the coastal seas without large river influence, OAH also occurs as a consequence of seasonal productivity and large-scale circulation processes. Along the Hokkaido coast, the highly euphotic Tokyo Bay, the Netarts Bay off Oregon, and the coastal habitat types on eastern Long Island, time series observations show the progression of seasonal OA and deoxygenation, often resulting in hypoxic conditions. In addition, high frequency pH and dissolved oxygen (DO) observations across sub-diel, diel and seasonal time scales across various habitat types (salt marsh, macroalgae, seagrass, open water) in the northeast US show the impact of ecosystem metabolism to modulate OAH (Wallace et al.). Comprehensive analysis of coastal observations suggests that pH and  $\Omega_{Ar}$  decreased by 0.2–0.6 and 1–2, respectively, via circulation and biogeochemical processes, where  $\Omega_{Ar}$  decreases can occur in the summer bottom waters and will be a common phenomenon in the near future in the eutrophic Tokyo Bay (Yamamoto-Kawai et al.). Fujii et al. and Fairchild and Hales separately showed that along the Hokkaido coast and in Netarts Bay along the Oregon coast,  $\Omega_{Ar}$  sometimes decreases to values below the threshold for significant negative impacts on some calcifiers (e.g., 1.1–1.5 for bivalve larvae, 1–1.5 for pteropods, and pH values of 7.6–7.8 for echinoderms and decapods; Bednaršek, Ambrose et al.; Bednaršek, Calosi, et al.; Bednaršek, Naish, et al.; Bednaršek et al., 2019). Continued oceanic uptake of carbon dioxide will continue to decrease pH and  $\Omega_{Ar}$ , with high-latitude surface waters expected to be fully undersaturated by the end of this century because of the natural low buffer capacity there (Feely et al., 2009; Steinacher et al., 2009).

Crossing these pH thresholds consistently occurs in salt marsh and seagrass habitats along with hypoxic conditions (Wallace et al.). Under the IPCC global warming and acidification scenarios,  $\Omega_{Ar}$  in some coastal environments will drop below these thresholds by 2090, indicating that critical thresholds may be crossed more frequently in the future and severely damage calcifiers and impact overall fisheries production (Tai et al.).

## OCEAN ACIDIFICATION AND HYPOXIA AT THE CHEMICAL-BIOLOGICAL INTERFACE

Under continuously decreasing pH and low dissolved oxygen conditions, there is a general concern that the local bottom waters and the underlying sediments could switch from hypoxic to anoxic conditions. For example, in the hypoxic northern Gulf of Mexico, low DO conditions in sediment did not promote anoxic diagenesis as anticipated, possibly linked to the reduction of bioturbation during the hypoxic spring and summer months (Rabouille et al.). In the hypoxic area of the Eastern Arabian Sea, strong denitrification results in large nitrogen loss, accounting for as much as 20–60% of the total annual fixed nitrogen loss in oxygen minimum zone of the Arabian Sea (Sarkar et al.). Methane emissions in coastal regions can also be very large,

accounting for as much as 15% of the methane emission from the Arabian Sea (Sudheesh et al.). Moreover, sediment diagenesis plays a critical role in triggering and maintaining hypoxia of lagoon waters, and it may be enhanced by changes in regional climate conditions, such as the increase in frequency of summer heat waves (Brigolin et al.).

## IMPACTS OF OCEAN ACIDIFICATION AND HYPOXIA ON MARINE ORGANISMS AND ECOSYSTEMS

OA and hypoxia are significant stressors for marine species, communities, ecosystems, especially when they act interactively and cumulatively. Studies show that harmful effects of OA on the marine calcifiers have already been observed. In the Arctic and subpolar Beaufort Sea, Bering Sea, and the Amundsen Gulf, corrosive water for aragonite induced extensive shell dissolution in ecologically important zooplankton, i.e., pteropods (Niemi et al.). Conducting a more comprehensive OA risk assessment, Bednaršek, Naish, et al. elucidated high exposure OA risk in combination with high sensitivity and low adaptive capacity for pteropods in the polar habitats of the Northern Hemisphere.

Thresholds are very useful tools to determine when the OA exposure can start causing negative physiological and organismal impairments. With the echinoderms and decapods being one of the most dominant as well as ecologically and economically important species, the application of the thresholds for these two groups can have important regional and global implications (Bednaršek, Ambrose, et al.; Bednaršek, Calosi, et al.). These thresholds provide the foundation for consistent interpretation of OA monitoring data or numerical ocean model simulations to support climate change marine vulnerability assessments and evaluation of ocean management strategies.

On longer time scales, model results indicate that OA amplifies multi-stressor impacts on global marine invertebrate fisheries, with the fish catch potential to decrease by 12%, with 3.4% being attributed to OA by the end of this century (Tai et al.). A comprehensive understanding of OA effects based on the thresholds and predictive sensitivities allows for improved predictions of ecosystem change relevant to effective fisheries resource management, as well as providing a more robust foundation for ecosystem health monitoring of the negative OA impacts in the most sensitive OAH habitats. While OA can also significantly affect the range of responses in different zooplankton taxa, the study by Keil et al. found little association between empirical measures of *in situ* pH and the abundance of sensitive taxa as revealed by meta-analysis. The authors concluded that the mismatch between experimental studies and field observations should have some important ramifications for the design of long-term monitoring programs and interpretation and use of the data produced.

On the community level, the results of mesocosms-based experiments across various marginal seas, from the coastal East China Sea, Bohai Sea, coastal upwelling and riverine ecosystems in Chile, all agree that increasing partial pressure of CO<sub>2</sub> (*p*CO<sub>2</sub>) can modulate plankton structure, composition and abundance, leading to altered biogeochemical cycles of carbon and nutrients, and carbon fluxes. Elevated *p*CO<sub>2</sub>

mesocosm experiments in the East China Sea boosted biomass of diatoms, while impeding the succession of diatoms to dinoflagellates, and corresponds with increased abundance of virus and bacteria (Huang R. et al.). Such results appear to be region specific, because a different community response was demonstrated in the Bohai Sea, where high *p*CO<sub>2</sub> resulted in the decreased total diatom abundance, favoring the ratio of central to pennate diatoms. In addition, combined warming and OA significantly decreased the proportion of diatoms to dinoflagellates and caused the shifts in phytoplankton composition due to interactive and cumulative effect, ultimately resulting in carbon flux and sinking rate changes (Feng et al.). Another study in the coastal area off Chile, characterized by high natural variability, showed no response to high *p*CO<sub>2</sub> treatments; instead the changes during the incubations were related to other factors, such as competition and growth phase (Osma et al.). The study suggests that the pre-exposure to variable coastal gradients that structure local adaptation patterns could play an important role in determining responses of coastal phytoplankton communities to increased impact of OA. In the experiments combining various OA and light treatments conducted on 15 laboratory experimental generations of picophytoplankton, Bao and Gao showed that *Synechococcus* grew faster under the OA treatment with inhibiting light level only, suggesting differential picophytoplankton responses that are light dependent under various depth conditions.

Hypoxia is another stressor present mostly in the tropical and temperate marine ecosystems. In a tropical Caribbean reef, hypoxia had largest negative impact on the performance of a key reef herbivore. The interactive temperature and DO extremes with low pH led to impaired performance of the reef echinoderms (Lucey et al.).

The studies investigating the impact of carbonate chemistry variability in coastal regions demonstrate the importance on both biological and biogeochemical responses. Coastal and estuarine habitats are characterized by distinct temporal fluctuations in carbonate chemistry, ranging from sub-diel to diel to seasonal, which are expected to increase under projected scenarios even in the highly buffered systems (Urbini et al.). Extreme variability in hypoxia/reoxygenation seem to change the expression of the mitochondrial quality control pathways only of the species with high DO sensitivity, such as Pacific oysters *Crassostrea gigas*, but not blue mussels *Mytilus edulis*, elucidating the mechanisms of mitochondrial protection against hypoxia-reoxygenation-induced damage that might contribute to hypoxia tolerance in marine bivalves (Steffen et al.). In addition to eutrophication, marine heatwave might also contribute to triggering deoxygenation and biodiversity loss in the marginal seas. In a southwestern Atlantic coast, marine heatwaves, sewage and eutrophication combined to trigger deoxygenation and biodiversity loss (Brauko et al.).

## LONG-TERM VARIABILITY IN OCEAN ACIDIFICATION AND HYPOXIA IN MARGINAL SEAS

In the marginal seas of the Indian Ocean (Persian Gulf, Red Sea and Andaman Sea), deoxygenation has been observed numerous

times over the last few decades (Naqvi). Hypoxia in the East China Sea has become more severe since the 1960s mainly due to eutrophication, stronger stratification, and longer water residence times (Wang et al.). ENSO and global warming may also have indirect effects by regulating river discharge, stratification, and water residence time, etc. (Wang et al.). In the southwestern English Channel within the Northeastern Atlantic Ocean, time-series observations show that average  $p\text{CO}_2$  increases at rate of  $2.95\text{--}3.52 \mu\text{atm yr}^{-1}$ , with a corresponding decrease in mean pH of  $0.0028 \text{ yr}^{-1}$  (Gac et al.), an acidification rate faster than the open ocean ( $\sim 1.5 \mu\text{atm yr}^{-1}$  for  $p\text{CO}_2$  and  $-0.0016 \sim -0.0017 \text{ yr}^{-1}$  for pH; Bates et al., 2014), and consistent with some other marginal seas, including the Mediterranean (Hassoun et al., 2015). Both atmospheric  $\text{CO}_2$  absorption and climatic indices (i.e., North Atlantic Oscillation and Atlantic Multidecadal Variability) are responsible for this fast OA rate in the northern East Atlantic Ocean (Gac et al.).

## CONCLUSIONS AND PERSPECTIVES

OA and hypoxia often occur more severely in the marginal seas than in the open ocean globally, making the marginal seas species and ecosystems more vulnerable to future climate change related changes.  $\Omega_{\text{Ar}}$  and pH conditions in some marginal seas are already below the thresholds that can induce negative biological responses for many marine calcifiers, especially in the rapidly changing polar/subpolar marginal seas or in coastal upwelling regions. In temperate marginal seas, subsurface water can be corrosive, which may be having an impact on fisheries and the ecosystem services they provide. For large river-dominated margins, there might be significant time lags of the bottom water hypoxia/acidification after the peak of the primary production. For coastal ecosystems in the margin systems characterized by the OA/hypoxia, we can expect differential effects and evolution across regional habitats, depending on the baseline and the physical and biogeochemical dynamics of local conditions. Understanding of such spatial and temporal variability is thus essential to start recognizing more sensitive habitats and conduct appropriate monitoring or management practices to protect and preserve ecologically and economically important ecosystems.

Marginal seas are productive areas essential for the human wellbeing and economic dependence, but insufficient awareness of biological and ecosystem responses and potential management strategies might be detrimental, especially in the developing countries. Although this Research Topic contributed to advance understanding of the chemical changes, the interpretation of biological responses in the marginal seas is still in need of more research. Such responses are complex, thus requiring a tight integration with the chemical and biogeochemical multi-scale parameters that can induce stress, community reorganization and shifts, biological interactions and others impacts.

An immediate need for enhanced understanding of multiple stressor effects as well as the effects of increased variability and unpredictability in the marginal seas systems is critical for developing better management strategies. While a single study indicates that multiple stressor extremes in the tropics

lead to the physiological impairments, systematic studies are needed to reveal multiple stressor impacts on the marginal seas marine ecosystems. Equally, the projections of future conditions in dynamic coastal systems show enhanced variability and extreme values related to OA, which can be habitat specific and thus extremely variable, yet biological and biogeochemical implications of these impacts are largely unknown. In particular, a better understanding of increased amplitude variability and prolonged duration below thresholds for organisms and ecosystems is needed for the coastal-estuarine habitat. Various temporal scales of variability (from sub-diel to diel to seasonal) needs to be further examined to understand where and when the biological bottlenecks will first occur. The comparison of sensitivity and resilience of various marginal seas systems should be examined through the natural variability baseline to understand the extent of species plasticity and adaptation. Moreover, attention needs to be given to the temporal variation (autocorrelation and cross-correlations) that represents the framework of the “predictability” in the habitats (Bernhardt et al., 2020), which can also significantly structure biological responses. Extensive theoretical and empirical work shows that the predictability might in fact be a primary driver determining the biological responses compared to the variability, thus both, predictability and variability require more attention to assess their impact and trade-offs in the marginal seas.

The integrated results of this Research Topic carry important implications for variety of ecosystems and ecosystem services, including aquaculture practices, fisheries management, human wellbeing carbon sequestration, etc. Given enormous potential of ecosystems services in the marginal seas systems, much more comprehensive approaches are needed to assess the impacts and economic evaluation of their losses. The approach needs to be based on the integration of the chemical, biological and biogeochemical data, allowing to monitor changes over time, and developing management approaches to preserve the health and the biodiversity within the marginal seas in the face of the global climate change, including habitat restoration, protection of biogenic habitats, removal of anthropogenic nutrients, potential development of OAH habitat refugia, marine spatial planning, fishing practices and capacity of adaptation and resilience of the changing socio-ecological system. Special attention needs to be given to the “blue carbon” ecosystems given their role related to sequestering carbon and potentially slowing down the long-term changes at the local level while also exacerbating short-term variability. To this end, a spatially targeted evaluation related to different causes of OAH involving comprehensive interactions with local stakeholders is needed maximize the utility of smaller-scale policy recommendations.

## AUTHOR CONTRIBUTIONS

All authors listed have made a substantial, direct, and intellectual contribution to the work and approved it for publication.

## FUNDING

This Research Topic was supported by the National Natural Science Foundation of China (41876080), the Strategic Priority Research Program of the Chinese Academy of Sciences (XDB42000000), and the NOAA Ocean Acidification Program. This is contribution number 5332 from the NOAA Pacific Marine Environmental

Laboratory. NB was supported by the Slovene Research Agency (J12468).

## ACKNOWLEDGMENTS

We thank the Frontiers in Marine Sciences editorial staff for their professional support. The peer-review team are appreciated for their insightful comments and suggestions.

## REFERENCES

- Andersson, A. J., Mackenzie, F. T., and Lerman, A. (2005). Coastal ocean and carbonate systems in the high CO<sub>2</sub> world of the anthropocene. *Am. J. Sci.* 305, 875–918. doi: 10.2475/ajs.305.9.875
- Bates, N. R., Astor, Y. M., Church, M. J., Currie, K., Dore, J. E., Gonzalez-Davila, M., et al. (2014). A time-series view of changing surface ocean chemistry due to ocean uptake of anthropogenic CO<sub>2</sub> and ocean acidification. *Oceanography* 27, 126–141. doi: 10.5670/oceanog.2014.16
- Bednaršek, N., Feely, R. A., Howes, E. L., Hunt, B. P. V., Kessouri, F., Leon, P., et al. (2019). Systematic review and meta-analysis toward synthesis of thresholds of ocean acidification impacts on calcifying pteropods and interactions with warming. *Front. Mar. Sci.* 6, 227. doi: 10.3389/fmars.2019.00227
- Bernhardt, J. R., O'Connor, M. I., Sunday, J. M., and Gonzalez, A. (2020). Life in fluctuating environments. *Philos. Trans. R. Soc. B Biol. Sci.* 375, 20190454. doi: 10.1098/rstb.2019.0454
- Cai, W.-J., Hu, X., Huang, W.-J., Murrell, M. C., Lehrter, J. C., Lohrenz, S. E., et al. (2011). Acidification of subsurface coastal waters enhanced by eutrophication. *Nat. Geosci.* 4, 766–770. doi: 10.1038/ngeo1297
- Carstensen, J., and Duarte, C. M. (2019). Drivers of pH variability in coastal ecosystems. *Environ. Sci. Technol.* 53, 4020–4029. doi: 10.1021/acs.est.8b03655
- Cohen, A. L., and Holcomb, M. (2009). Why corals care about ocean acidification: Uncovering the mechanism. *Oceanography* 22, 118–127. doi: 10.5670/oceanog.2009.102
- Doney, S. C. (2006). The dangers of ocean acidification. *Sci. Am.* 294, 58–65. doi: 10.1038/scientificamerican0306-58
- Doney, S. C., Busch, D. S., Cooley, S. R., and Kroeker, K. J. (2020). The impacts of ocean acidification on marine ecosystems and reliant human communities. *Annu. Rev. Environ. Resour.* 45, 83–112. doi: 10.1146/annurev-environ-012320-083019
- Doney, S. C., Fabry, V. J., Feely, R. A., and Kleypas, J. A. (2009). Ocean acidification: The other CO<sub>2</sub> problem. *Ann. Rev. Mar. Sci.* 1, 169–192. doi: 10.1146/annurev.marine.010908.163834
- Ekstrom, J. A., Suatoni, L., Cooley, S. R., Pendleton, L. H., Waldbusser, G. G., Cinner, J. E., et al. (2015). Vulnerability and adaptation of US shellfisheries to ocean acidification. *Nat. Clim. Chang.* 5, 207–214. doi: 10.1038/nclimate2508
- Feely, R. A., Alin, S. R., Carter, B., Bednaršek, N., Hales, B., Chan, F., et al. (2016). Chemical and biological impacts of ocean acidification along the west coast of North America. *Estuar. Coast. Shelf Sci.* 183, 260–270. doi: 10.1016/j.ecss.2016.08.043
- Feely, R. A., Alin, S. R., Newton, J., Sabine, C. L., Warner, M., Devol, A., et al. (2010). The combined effects of ocean acidification, mixing, and respiration on pH and carbonate saturation in an urbanized estuary. *Estuar. Coast. Shelf Sci.* 88, 442–449. doi: 10.1016/j.ecss.2010.05.004
- Feely, R. A., Doney, S. C., and Cooley, S. R. (2009). Ocean acidification: Present conditions and future changes in a high-CO<sub>2</sub> world. *Oceanography* 22, 36–47. doi: 10.5670/oceanog.2009.95
- Feely, R. A., Okazaki, R. R., Cai, W.-J., Bednaršek, N., Alin, S. R., Byrne, R. H., et al. (2018). The combined effects of acidification and hypoxia on pH and aragonite saturation in the coastal waters of the California current ecosystem and the northern Gulf of Mexico. *Cont. Shelf Res.* 152, 50–60. doi: 10.1016/j.csr.2017.11.002
- Feely, R. A., Sabine, C. L., Hernandez-Ayon, J. M., Ianson, D., and Hales, B. (2008). Evidence for upwelling of corrosive “acidified” water onto the continental shelf. *Science* 320, 1490–1492. doi: 10.1126/science.1155676
- Feely, R. A., Sabine, C. L., Lee, K., Berelson, W., Kleypas, J., Fabry, V. J., et al. (2004). Impact of anthropogenic CO<sub>2</sub> on the CaCO<sub>3</sub> system in the oceans. *Science* 305, 362–366. doi: 10.1126/science.1097329
- Gattuso, J. P., Magnan, A., Bille, R., Cheung, W. W. L., Howes, E. L., Joos, F., et al. (2015). Contrasting futures for ocean and society from different anthropogenic CO<sub>2</sub> emissions scenarios. *Science* 349, aac4722. doi: 10.1126/science.aac4722
- Green, R. E., Bianchi, T. S., Dagg, M. J., Walker, N. D., and Breed, G. A. (2006). An organic carbon budget for the Mississippi River turbidity plume and plume contributions to air-sea CO<sub>2</sub> fluxes and bottom water hypoxia. *Estuar. Coasts* 29, 579–597. doi: 10.1007/BF02784284
- Hassoun, A. E. R., Gemayel, E., Krasakopoulou, E., Goyet, C., M., Saab, A.-A., et al. (2015). Acidification of the Mediterranean Sea from anthropogenic carbon penetration. *Deep Sea Res. Part I Oceanogr. Res. Pap.* 102, 1–15. doi: 10.1016/j.dsr.2015.04.005
- Howarth, R., Chan, F., Conley, D. J., Garnier, J., Doney, S. C., Marino, R., et al. (2011). Coupled biogeochemical cycles: Eutrophication and hypoxia in temperate estuaries and coastal marine ecosystems. *Front. Ecol. Environ.* 9, 18–26. doi: 10.1890/100008
- Kleypas, J. A., and Yates, K. K. (2009). Coral reefs and ocean acidification. *Oceanography* 22, 108–117. doi: 10.5670/oceanog.2009.101
- Li, D. J., Zhang, J., Huang, D. J., Wu, Y., and Liang, J. (2002). Oxygen depletion off the Changjiang (Yangtze River) estuary. *Sci. China Ser. D Earth Sci.* 45, 1137–1146. doi: 10.1360/02yd9110
- Riebesell, U., Zondervan, I., Rost, B., Tortell, P. D., Zeebe, R. E., and Morel, F. M. M. (2000). Reduced calcification of marine plankton in response to increased atmospheric CO<sub>2</sub>. *Nature* 407, 364–367. doi: 10.1038/35030078
- Steinacher, M., Joos, F., Froelicher, T. L., Plattner, G. K., and Doney, S. C. (2009). Imminent ocean acidification in the Arctic projected with the NCAR global coupled carbon cycle-climate model. *Biogeosciences* 6, 515–533. doi: 10.5194/bg-6-515-2009
- Wang, H., Dai, M., Liu, J., Kao, S.-J., Zhang, C., Cai, W.-J., et al. (2016). Eutrophication-driven hypoxia in the East China Sea off the Changjiang estuary. *Environ. Sci. Technol.* 50, 2255–2263. doi: 10.1021/acs.est.5b06211
- Zhu, Z.-Y., Wu, H., Liu, S.-M., Wu, Y., Huang, D.-J., Zhang, J., et al. (2017). Hypoxia off the Changjiang (Yangtze River) estuary and in the adjacent East China Sea: quantitative approaches to estimating the tidal impact and nutrient regeneration. *Mar. Pollut. Bull.* 125, 103–114. doi: 10.1016/j.marpolbul.2017.07.029

**Conflict of Interest:** The authors declare that the research was conducted in the absence of any commercial or financial relationships that could be construed as a potential conflict of interest.

**Publisher's Note:** All claims expressed in this article are solely those of the authors and do not necessarily represent those of their affiliated organizations, or those of the publisher, the editors and the reviewers. Any product that may be evaluated in this article, or claim that may be made by its manufacturer, is not guaranteed or endorsed by the publisher.

Copyright © 2022 Guo, Bednaršek, Wang, Feely and Laurent. This is an open-access article distributed under the terms of the Creative Commons Attribution License (CC BY). The use, distribution or reproduction in other forums is permitted, provided the original author(s) and the copyright owner(s) are credited and that the original publication in this journal is cited, in accordance with accepted academic practice. No use, distribution or reproduction is permitted which does not comply with these terms.



# Comparing Subsurface Seasonal Deoxygenation and Acidification in the Yellow Sea and Northern East China Sea Along the North-to-South Latitude Gradient

Tian-qi Xiong<sup>1</sup>, Qin-sheng Wei<sup>2,3</sup>, Wei-dong Zhai<sup>1\*</sup>, Cheng-long Li<sup>1</sup>, Song-yin Wang<sup>1</sup>, Yi-xing Zhang<sup>1</sup>, Shuo-jiang Liu<sup>1</sup> and Si-qing Yu<sup>1</sup>

## OPEN ACCESS

### Edited by:

Nina Bednarsek,  
Southern California Coastal Water  
Research Project, United States

### Reviewed by:

Stephen F. Gonski,  
University of Delaware, United States  
Wen-Chen Chou,  
National Taiwan Ocean University,  
Taiwan  
Jianzhong Su,  
Xiamen University, China

### \*Correspondence:

Wei-dong Zhai  
wdzhai@126.com

### Specialty section:

This article was submitted to  
Coastal Ocean Processes,  
a section of the journal  
Frontiers in Marine Science

**Received:** 28 May 2020

**Accepted:** 28 July 2020

**Published:** 18 August 2020

### Citation:

Xiong T, Wei Q, Zhai W, Li C,  
Wang S, Zhang Y, Liu S and Yu S  
(2020) Comparing Subsurface  
Seasonal Deoxygenation  
and Acidification in the Yellow Sea  
and Northern East China Sea Along  
the North-to-South Latitude Gradient.  
*Front. Mar. Sci.* 7:686.  
doi: 10.3389/fmars.2020.00686

<sup>1</sup> Institute of Marine Science and Technology, Shandong University, Qingdao, China, <sup>2</sup> First Institute of Oceanography, Ministry of Natural Resources, Qingdao, China, <sup>3</sup> Laboratory for Marine Ecology and Environmental Science, Qingdao National Laboratory for Marine Science and Technology, Qingdao, China

To better understand the relationship between subsurface seasonal deoxygenation and acidification in the Yellow Sea and northern East China Sea (ECS), we examined carbonate system parameters and dissolved oxygen (DO) of seven field surveys conducted in 2017–2018, spanning all four seasons. Low  $pH_T$  values of 7.71–7.80 and critically low aragonite saturation state ( $\Omega_{arag}$ ) values of 1.07–1.40 along with undersaturated DO of mostly higher than 150  $\mu\text{mol O}_2 \text{ kg}^{-1}$  occurred in the Yellow Sea Cold Water Mass area in summer and autumn, while hypoxic DO values of 49–63  $\mu\text{mol O}_2 \text{ kg}^{-1}$  and extremely low  $pH_T$  values of 7.68–7.74 as well as critically low  $\Omega_{arag}$  values of 1.21–1.39 were observed in the northern ECS in July 2018. At the beginning of warm-season stratification formation, the cold Yellow Sea waters had much higher DO but lower  $\Omega_{arag}$  values than those in relatively warmer ECS waters, while yearly initial  $pH_T$  values rarely exhibited differences between the two coastal seas. During warm seasons, the central Yellow Sea accumulated respiration products beneath the thermocline in summer and autumn, while the northern ECS bottom waters preserved them only in summer. This study highlights fundamental roles of wintertime carbon dioxide ( $\text{CO}_2$ ) solubility along a north-to-south latitude gradient in the coastal acidification development. In comparison with the relatively low-latitude northern ECS subject to seasonal hypoxia, relatively high-latitude Yellow Sea exhibits higher  $\text{CO}_2$  solubility in winter and longer respiration-product accumulations in warm seasons, leading to lower  $\Omega_{arag}$  in the central Yellow Sea than those in the northern ECS. However, the present-day central Yellow Sea is free from hypoxia.

**Keywords:** coastal acidification, hypoxia, carbon dioxide solubility, community respiration, Yellow Sea, northern East China Sea

## KEY POINTS

- Wintertime air-sea re-equilibration, summertime respiration and autumnal upset dominate subsurface carbonate chemistry in coastal seas.
- High CO<sub>2</sub> solubility together with respiration leads to high DIC:TALK ratios and low aragonite saturation state in the central Yellow Sea.
- The northern East China Sea is subject to concurrent hypoxia and CO<sub>2</sub> acidification in summer, while the Yellow Sea is free from hypoxia.

## INTRODUCTION

The oceanic absorption of anthropogenic carbon dioxide (CO<sub>2</sub>) has lowered sea surface pH and calcium carbonate (CaCO<sub>3</sub>) mineral saturation state ( $\Omega$ ) as compared with the preindustrial era, known as ocean acidification (Caldeira and Wickett, 2003; Orr et al., 2005; Doney et al., 2009). Here pH is the negative logarithm of the sum of the concentrations of hydrogen (H<sup>+</sup>) and bisulfate (HSO<sub>4</sub><sup>-</sup>) ions, i.e., total hydrogen ion concentration scale,  $\text{pH}_T = -\log_{10}[\text{H}^+]_T$ , where  $[\text{H}^+]_T = [\text{H}^+] + [\text{HSO}_4^-]$ . It affects chemical/biochemical properties of seawater, including chemical reactions, equilibrium conditions, and biological toxicity.  $\Omega$  is defined as  $[\text{Ca}^{2+}] \times [\text{CO}_3^{2-}]/K_{\text{sp}}^*$ , where  $[\text{Ca}^{2+}]$  and  $[\text{CO}_3^{2-}]$  are the concentrations of calcium and carbonate ions, respectively, and  $K_{\text{sp}}^*$  is the apparent solubility product for either calcite or aragonite. The declines in pH and  $\Omega$  could lead to CaCO<sub>3</sub>-undersaturated corrosive seawater conditions, affecting marine calcifying organisms and even the whole marine ecosystem (Fabry, 2008; Jin et al., 2015; Ravaglioli et al., 2020).

The anthropogenic CO<sub>2</sub> invasion has resulted in a decrease in pH by 0.1 unit (Orr et al., 2005) and a decline in  $[\text{CO}_3^{2-}]$  by 30% (Sabine et al., 2004) in the upper ocean since the industrial revolution. The present-day open ocean pH<sub>T</sub> was detected at  $8.023 \pm 0.004$  in the tropical Central Pacific (6.4°N 162.4°W), at  $8.074 \pm 0.004$  in the subtropical Eastern Pacific (33.5°N 122.5°W), and at  $8.020 \pm 0.008$  at an Antarctic site (77.6°S 166.4°W) (Hofmann et al., 2011). In the Pacific Ocean, the present surface  $\Omega_{\text{arag}}$  values are 3–4.5 in low-latitude regions while only 1–2 in high-latitude regions (Feely et al., 2012). This latitude gradient of  $\Omega_{\text{arag}}$  is largely attributed to higher solubility of CO<sub>2</sub> in colder seawaters of high-latitude regions. Moreover, seasonal aragonite undersaturation (i.e.,  $\Omega_{\text{arag}} < 1$ ) has already been observed in surface and shallow subsurface waters of some northern polar seas (Bates et al., 2009; Fabry et al., 2009; Qi et al., 2017).

Chemically,  $\Omega_{\text{arag}} > 1$  indicates that the CaCO<sub>3</sub> mineral of aragonite is stable in the seawater, while  $\Omega_{\text{arag}} < 1$  indicates that the mineral is unstable. Although corals usually require much higher  $\Omega_{\text{arag}}$  of  $> 3.0$  for optimal growth (Eyre et al., 2018; Yamamoto A. et al., 2012), many researchers regarded an  $\Omega_{\text{arag}}$  value of 1.5 as a critical threshold for marine shellfish development (Gruber et al., 2012; Ekstrom et al., 2015; Waldbusser et al., 2015), below which marine calcifying

organisms may be under threat of acidified seawaters. On the Chinese side of the North Yellow Sea, the net community calcification rate in subsurface waters declined to zero when the  $\Omega_{\text{arag}}$  value reached the critical level of 1.5–1.6 (Li, 2019; Li and Zhai, 2019).

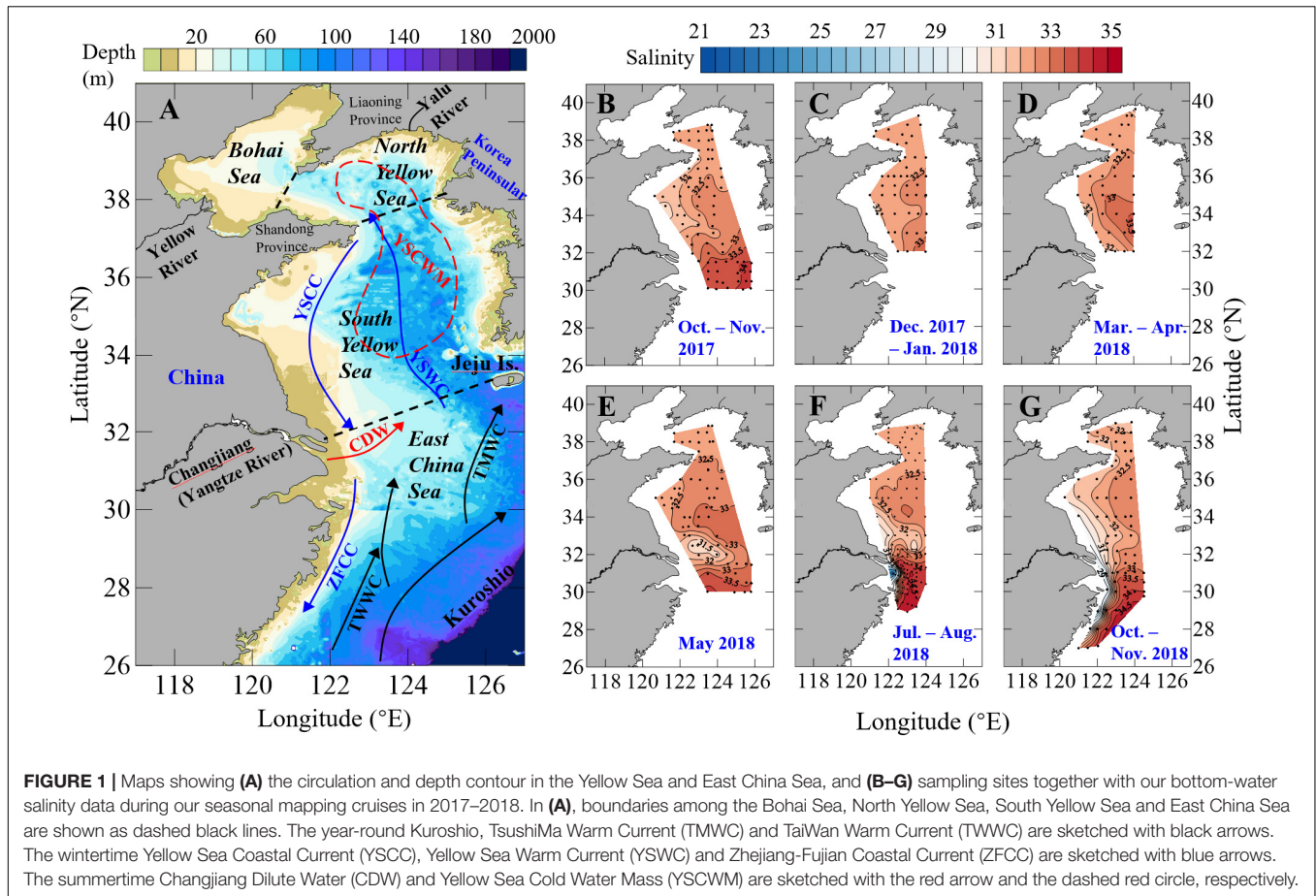
In productive coastal zones, algae and other biogenic particles decompose in subsurface waters. Their respiration and/or remineralization processes consume dissolved oxygen (DO) and release a great deal of CO<sub>2</sub> into subsurface waters, leading to more rapid seawater acidification in coastal seas, compared with the open ocean (Feely et al., 2010; Cai et al., 2011; Melzner et al., 2013; Jiang et al., 2019). Moreover, the respiration-induced seasonal acidification is subject to uneven distributions of seawater temperature, salinity and alkalinity in coastal seas. For example, transregional carbonate studies along the U.S. East Coast have indicated that its northeast shelf region is more susceptible to CO<sub>2</sub> acidification than the southern region, along with a north-to-south increasing gradient in total alkalinity (TALK) and limited geographical variation in dissolved inorganic carbon (DIC) (Wang et al., 2013; Wanninkhof et al., 2015). Exposure, sensitivity and adaptive capacity to the acidification driven by atmospheric CO<sub>2</sub> absorption and local amplifiers (i.e., eutrophication, upwelling of CO<sub>2</sub>-riched waters and input of river water with low  $[\text{Ca}^{2+}]$  and subsequently  $\Omega_{\text{arag}}$ ) were also assessed and compared throughout the U.S. coastal regions (Ekstrom et al., 2015). Along China's coasts, so far, the latitude gradient of coastal acidification and its controlling mechanisms are unclear because previous studies have been primarily confined to individual coastal seas (e.g., Cao et al., 2011; Chou et al., 2013a; Zhai, 2018). Ocean environments along China's coasts also exhibit complex local geological and hydrological characteristics, such as contrasting bottom topography, residence time and monsoon-driven coastal currents (e.g., Su and Yuan, 2005; Chen, 2009; Men and Liu, 2015).

In this study, we examined carbonate system parameters in the Yellow Sea and northern East China Sea (ECS) during 2017–2018, spanning all four seasons. For the first time, a north-to-south gradient of carbonate system parameters in contrasting coastal seas along China's east coast was revealed. Together with hydrological data and DO measurements, the regional differentiation of the respiration-induced coastal acidification in the two coastal seas were investigated. This study provides the best understanding so far of the relationship between subsurface seasonal deoxygenation and acidification in the two coastal seas of both ecological and economic importance, which will assist future predictions of marine environmental changes under ocean acidification in the coming decades.

## MATERIALS AND METHODS

### Study Area

The Yellow Sea and ECS, located on the China eastern shelf, are two major marginal seas of the western North Pacific. The boundary of the two coastal seas lies between the northern corner of the Changjiang Estuary and Jeju Island (**Figure 1A**). The Yellow Sea is surrounded by mainland China to the west and the



Korea Peninsula to the east. It is geographically divided into two basins, i.e., the North Yellow Sea and the South Yellow Sea. The former is connected to the Bohai Sea to the west, and the latter to the ECS to the south. The North Yellow Sea has an area of  $\sim 7 \times 10^4 \text{ km}^2$  with an average water depth of  $\sim 38 \text{ m}$ , while the South Yellow Sea has an area of  $\sim 30 \times 10^4 \text{ km}^2$  with an average water depth of  $\sim 44 \text{ m}$ . The more open ECS has a larger area of  $\sim 77 \times 10^4 \text{ km}^2$  with an average water depth of  $\sim 370 \text{ m}$ . The ECS inner shelf within the 50 m isobaths is quite broad. The climatic variations are primarily dominated by the East Asian Monsoon, with the rain-bearing southwest monsoon prevailing in summer (from June to early September) and a strong northeast monsoon lasting in winter (from December to early March of the next year, Chen, 2009).

Both of the ECS and the Yellow Sea are connected to the North Pacific via the Kuroshio intrusion, including those Kuroshio-derived currents such as the TaiWan Warm Current (TWWC), the TsushiMa Warm Current (TMWC), and the Yellow Sea Warm Current (YSWC). Moreover, they are subject to freshwater discharges from the Changjiang and Yalu Rivers (Figure 1A), as well as several monsoon-driving coastal currents, including the northeastward-moving Changjiang Diluted Water (CDW) from late spring to early autumn, and the southward-moving Yellow Sea Coastal Current (YSCC) and Zhejiang-Fujian Coastal Current (ZFCC) in winter and early spring.

The Yellow Sea is semi-enclosed. Its summertime hydrography is characterized by a pronounced stratification in its deeper regions. A cold pool with water temperatures of  $5\text{--}11^\circ\text{C}$ , the Yellow Sea Cold Water Mass (YSCWM), develops under the thermocline from late spring to autumn as the remnant of the previous winter cooling (Miao et al., 1990; Zhai et al., 2014b). The wintertime hydrography in the Yellow Sea is characterized by the southward-moving YSCC and the northward-moving YSWC (Figure 1A). The YSWC is considered to be a compensating current to the monsoon-driven coastal current (Yuan et al., 2008), transporting warm and saline waters into the Yellow Sea. Based on  $^{228}\text{Ra}/^{226}\text{Ra}$  measurements, the Yellow Sea hydraulic residence time has been estimated to be 5–6 years, while the residence time may only be 2–3 years or shorter on the ECS shelf (Nozaki et al., 1991; Men and Liu, 2015).

TALK in the Yalu River is only  $320\text{--}800 \mu\text{mol kg}^{-1}$  (Zhai et al., 2014b, 2015), approximately  $1000 \mu\text{mol kg}^{-1}$  lower than the Changjiang TALK value ( $1500\text{--}1900 \mu\text{mol kg}^{-1}$ , Xiong et al., 2019). As illustrated by Chen and Wang (1999) and Zhai et al. (2014a), the ECS offshore waters originate from the Kuroshio tropical water. The latter has a typical TALK value of  $2293 \mu\text{mol kg}^{-1}$  and the DIC value of  $1994 \mu\text{mol kg}^{-1}$  (with the DIC:TALK ratio of  $< 0.9$ ) at a salinity of 34.9 (Chen and Wang, 1999). By comparison, the TALK values in the semi-enclosed Yellow Sea were usually detected in a compact range of  $2290 \pm 25 \mu\text{mol kg}^{-1}$

(Zhai, 2018). In the North Yellow Sea, a usual water mixing model has been reported by Zhai et al. (2014b), i.e.,

$$\text{TALK}^{\text{North\_Yellow\_Sea}} = 61.745 \times \text{Salinity} + 320 \quad (1)$$

where 320 ( $\mu\text{mol kg}^{-1}$ ) represents the low TALK feature of the mixture of rainwater and freshwater discharged from the Yalu River.

## Sampling and Analyses

In this study, seven field surveys were conducted on the Chinese side of the Yellow Sea and the northern ECS during 2017–2018 (**Supplementary Table S1**), spanning a wet summer (July–August 2018) and a dry winter (December 2017–January 2018), as well as those transitional seasons of spring (March–May 2018) and autumn (October–November 2017 and October–November 2018) (**Figures 1B–G** and **Supplementary Figure S1A**).

Water samples were collected at two to seven different depths (including sea surface and the bottom water) using a rosette of 10 or 12 Niskin bottles, integrated with Conductivity-Temperature-Depth/Pressure (CTD) sensor packages. The ancillary data of *in situ* temperature (after the International Temperature Scale of 1990) and salinity (after the Practical Salinity Scale of 1978) were obtained primarily using the calibrated CTD sensor packages (SBE-19 plus in our October–November 2017 and May 2018 cruises, and SBE-911 plus during the other cruises, Sea-Bird Scientific, Bellevue, WA, United States). During the summertime estuarine survey conducted in July 2018, salinity values of discrete samples were also measured using a calibrated WTW's TetrCon925 probe.

DO samples were collected, fixed and titrated aboard following the Winkler procedure at an overall uncertainty level of <0.5%. A small quantity of sodium azide ( $\text{NaN}_3$ ) was added during subsample fixation to remove possible interferences from nitrites (Wong, 2012). The DO saturation (DO%) was calculated from field-measured DO concentration divided by the DO concentration at equilibrium with the atmosphere which was calculated from temperature, salinity and local air pressure, as per the Benson and Krause (1984) equation. To quantify the effect of net community metabolism, apparent oxygen utilization (AOU) was also calculated by subtracting the field-measured DO concentration from the air-equilibrated DO. Assuming the water starts with a fully saturated state, and ignoring effects of air-sea exchange and water mixing, an  $\text{AOU} > 0$  implies net community respiration, while an  $\text{AOU} < 0$  implies net community production.

Water samples for DIC and TALK analyses were also collected aboard. As recommended by Huang et al. (2012), water samples for DIC and TALK were stored in 60 mL borosilicate glass bottles (for DIC, bubble free) and 140 mL high-density polyethylene bottles (for TALK). There were no statistical differences between the measuring results from the above-mentioned sample storing procedure and from those procedure suggested by Dickson et al. (2007). Following filling procedure in Dickson et al. (2007), we filled these triple-rinsed sample bottles of DIC and TALK smoothly from the bottom, and then immediately

added 50  $\mu\text{L}$  of saturated mercuric chloride ( $\text{HgCl}_2$ ). Finally, water samples for DIC and TALK were sealed and preserved at room temperature until determination. Note that the volume of saturated  $\text{HgCl}_2$  added to the DIC samples exceeded the upper limit of recommended range (0.02–0.05% by volume), but was still below the maximum amount, i.e., 0.1% by volume (Dickson et al., 2007). Both DIC and TALK samples were unfiltered but allowed to settle before measurement, although filtration techniques suitable for these samples were reported earlier by Bockmon and Dickson (2014). DIC was measured by an infrared  $\text{CO}_2$  detector-based DIC analyzer (AS-C3, Apollo SciTech Inc., United States), and TALK was determined at 25°C by the Gran acidimetric titration using a semi-automated titrator (AS-ALK2, Apollo SciTech Inc., United States). DIC and TALK determinations were referred to Certificated Reference Materials (CRM) from Andrew G. Dickson's lab at Scripps Institution of Oceanography at a precision of  $\pm 2 \mu\text{mol kg}^{-1}$  (Dickson et al., 2007; Zhai et al., 2014b).

## Calculation of Other Carbonate System Parameters

Seawater fugacity of  $\text{CO}_2$  ( $f\text{CO}_2$ ),  $\text{pH}_T$  and  $\Omega_{\text{arag}}$  were calculated from seawater temperature, salinity, and measured DIC and TALK using the software CO2SYS.XLS (Version 24) (Pelletier et al., 2015), which is an updated version of the original CO2SYS.EXE (Lewis and Wallace, 1998). This program has been favorably evaluated by Orr et al. (2015) in a study comparing 10 packages of carbonate calculation program. The Millero et al. (2006) dissociation constants of carbonic acid were used in the calculation because they cover much broader applicable ranges of temperature (0–50°C) and salinity (0–50). The Dickson (1990) dissociation constant was used for  $\text{HSO}_4^-$  ion. The phosphate and silicate values required by the program were usually unavailable and replaced by zero. The  $\text{Ca}^{2+}$  concentrations were assumed to be proportional to salinity as presented in Millero (1979) and the values of apparent solubility product for aragonite ( $K_{\text{sp}}^*_{\text{arag}}$ ) were taken from Mucci (1983).

To assess the quality of the carbonate system data, we calculated pH data using the National Bureau of Standards scale ( $\text{pH}_{\text{NBS}}$ ) based on field-measured DIC and TALK values. These data were compared with field-measured  $\text{pH}_{\text{NBS}}$  data (see collection and analysis of  $\text{pH}_{\text{NBS}}$  samples in **Supplementary Material**). Most measured and calculated values were consistent at a deviation level of  $\pm 0.05 \text{ pH}$  (**Supplementary Figure S2A**). To examine the possible existences of organic alkalinity in coastal waters within our study area, we also calculated TALK values from field-measured DIC and  $\text{pH}_{\text{NBS}}$  data. Most measured TALK data and calculated results were consistent with each other at a deviation level of  $\pm 20 \mu\text{mol kg}^{-1}$  (**Supplementary Figure S2B**). This deviation level was reasonably higher than the precision of TALK determination ( $\pm 2 \mu\text{mol kg}^{-1}$ ). These comparisons suggested that the measured and calculated results of the carbonate system parameters were reliable. Due to accidentally insufficient addition of  $\text{HgCl}_2$ , the North Yellow Sea DIC samples collected in April 2018 were damaged before determination. The

relevant DIC data were calculated from field-measured TALK and  $\text{pH}_{\text{NBS}}$ .

To quantify the effect of net community metabolism on DIC, we calculated the air-equilibrated DIC (corresponding to a mean air-equilibrated  $f\text{CO}_2$  value of  $415 \pm 5 \mu\text{atm}$  during our seasonal cruises conducted in 2017–2018) from corresponding field-measured seawater temperature, salinity and TALK (Zhai, 2018). The air-equilibrated  $f\text{CO}_2$  was calculated from the flask analysis data of atmospheric  $\text{CO}_2$  mole fraction at the adjacent Tae-ahn Peninsula (TAP) site ( $36^\circ 44' \text{N}$   $126^\circ 08' \text{E}$ ), which varied from 406 ppm (ppm = parts of  $\text{CO}_2$  per million dry air) in August to 419–421 ppm during January to May in 2017–2018 (Supplementary Figure S1B, data from NOAA/ESRL's Global Monitoring Division)<sup>1</sup>, and corrected to the survey-based barometric pressure and 100% humidity at water temperature and salinity (Zhai et al., 2019). Similar to the definition of AOU (section "Sampling and Analyses"), the DIC departure from the air-equilibrated DIC was defined as the excess DIC (ExcessDIC). Assuming water starts with a fully saturated state, and ignoring effects of air-sea exchange, water mixing and  $\text{CaCO}_3$  precipitation/dissolution, an ExcessDIC > 0 means net community respiration, while an ExcessDIC < 0 implies net community production.

## RESULTS

### Hydrological Settings

Generally, water temperature exhibited a north-to-south-increasing gradient from the North Yellow Sea, to the South Yellow Sea, and to the northern ECS in winter, spring and autumn (Supplementary Figures S3–S5). The only exception was sea surface temperature in summer, showing no latitude gradient in these sea areas. However, summertime temperature in subsurface and bottom waters exhibited a north-to-south-increasing gradient (Supplementary Figures S4, S5). During our winter and spring cruises, regionally survey-averaged temperatures were  $4.8\text{--}7.8^\circ\text{C}$  in the North Yellow Sea,  $7.2\text{--}11.7^\circ\text{C}$  in the South Yellow Sea and  $9.6\text{--}16.7^\circ\text{C}$  in the northern ECS (Table 1).

Salinity also exhibited the north-to-south-increasing gradient, with annual mean values of  $32.1 \pm 0.3$  in the North Yellow Sea,  $32.2 \pm 0.7$  in the South Yellow Sea and  $32.6 \pm 1.9$  in the northern ECS, based on data obtained from our seasonal cruises in 2017–2018. The Yellow Sea had relatively low salinity values and small salinity variations as compared with the northern ECS (Figures 1B–G, 2A–C). In the Yellow Sea, relatively high salinity values of > 32 dominated the whole study area in winter and spring (Figures 1C–E). In summer and autumn, the relatively high salinity values of > 32 still dominated bottom waters in the central Yellow Sea (Figures 1B,F–G), i.e., the summertime YSCWM area (Figure 1A). In the connection between the northern ECS and South Yellow Sea, several low salinity values of 29.7–31.5 were observed in late spring (Figure 1E), likely due to the offshore transport of the CDW. In summer, the

CDW-affected sampling sites considerably increased, covering the northwestern ECS and the southern part of the South Yellow Sea (Figure 1F and Supplementary Figure S1A). In autumn, low salinity values of 26.1–30.5 were observed at nearshore stations in the ECS (Figure 1G), indicating the effect of the southward-moving ZFCC during this northeast monsoon-driven season (Figure 1A).

In the Yellow Sea, significant thermoclines and stratification occurred in summer and autumn (Figures 3A–C), with mean surface temperatures of  $26.7 \pm 2.3^\circ\text{C}$  and  $19.2 \pm 1.7^\circ\text{C}$  in summer and autumn, respectively, and with mean bottom-water temperatures of  $12.5 \pm 6.2^\circ\text{C}$  and  $13.9 \pm 4.7^\circ\text{C}$  in summer and in autumn, respectively (Supplementary Figure S6). In the central Yellow Sea, subsurface water had quite low temperature of  $\sim 9^\circ\text{C}$  in warm seasons (Figures 2A,B), shaping the YSCWM area with large density difference between bottom and surface waters ( $\Delta\text{Density}$ ) of  $\sim 5 \text{ kg m}^{-3}$  in summer and  $\sim 2 \text{ kg m}^{-3}$  in autumn (Figures 3A–C). Compared with the Yellow Sea, the northern ECS had relatively small bottom-surface temperature differences ( $26.1 \pm 1.8^\circ\text{C}$  versus  $20.9 \pm 1.7^\circ\text{C}$ ) and  $\Delta\text{Density}$  ( $3.7 \pm 1.8 \text{ kg m}^{-3}$ ) in summer, and nearly homogenous vertical profiles in autumn, except for several southeastern stations with bottom-water temperatures of  $19.9\text{--}23.7^\circ\text{C}$  and  $\Delta\text{Density}$  of  $0.4\text{--}2.1 \text{ kg m}^{-3}$  in October 2018 (Figures 3A–C and Supplementary Figure S6).

### DO and Carbonate System Parameters

#### DO, $f\text{CO}_2$ , and Apparent DO Depletion Rate

During our winter and spring cruises, most DO values were at  $\sim 100\%$  saturations, while  $f\text{CO}_2$  were close to the present-day air-equilibrated  $f\text{CO}_2$  of  $415 \mu\text{atm}$  in the Yellow Sea and northern ECS (Table 1 and Figures 2D–F), suggesting a vertically well-mixed situation during cold seasons. Exceptions to this were observed in the central part of the South Yellow Sea in winter, where relatively low DO% of 65–72% and supersaturated  $f\text{CO}_2$  of 672–806  $\mu\text{atm}$  occurred in bottom waters at four deep stations (Supplementary Figure S5). From late spring to autumn, the YSCWM bottom waters exhibited DO declines (from 97% or 285  $\mu\text{mol O}_2 \text{ kg}^{-1}$  in late spring to 87% or 248  $\mu\text{mol O}_2 \text{ kg}^{-1}$  in summer and 68% or 195  $\mu\text{mol O}_2 \text{ kg}^{-1}$  in autumn) and  $f\text{CO}_2$  increases (from 440  $\mu\text{atm}$  in late spring to 505  $\mu\text{atm}$  in summer and 680  $\mu\text{atm}$  in autumn) (Figures 2D,E, 3D–F). These low DO values in the YSCWM (mostly higher than 150  $\mu\text{mol O}_2 \text{ kg}^{-1}$ ) were still above the threshold of hypoxia (i.e., <63  $\mu\text{mol O}_2 \text{ kg}^{-1}$ ). The regional averaged apparent DO depletion rate in the YSCWM bottom waters was estimated to be 0.6  $\mu\text{mol O}_2 \text{ kg}^{-1} \text{ d}^{-1}$  from late spring to autumn ( $\sim 150$  days).

In the northern ECS, summertime bottom-water DO% values were averaged at only  $56 \pm 13\%$  (with a range of 21–84%, having the DO concentrations of 49–185  $\mu\text{mol O}_2 \text{ kg}^{-1}$ ), while the autumnal bottom-water DO% increased to the air-equilibrated level (Figures 2F, 3D–F). The three summertime hypoxic stations (with DO values of 49–63  $\mu\text{mol O}_2 \text{ kg}^{-1}$ ) off the Changjiang Estuary had extremely high  $f\text{CO}_2$  values of  $\sim 1000 \mu\text{atm}$  (Supplementary Figure S5). Since water stratification in the northern ECS was intensified from late spring to summer

<sup>1</sup><http://www.esrl.noaa.gov/gmd/>

**TABLE 1** | Summary of field data of water temperature, salinity, DO saturation (DO%) and carbonate system parameters<sup>a</sup>.

Season	Region	Sampling period	Temperature (°C)	Salinity	DO%	TAlk ( $\mu\text{mol kg}^{-1}$ )	DIC ( $\mu\text{mol kg}^{-1}$ )	DIC:TAlk ratio	pH <sub>T</sub> ( <i>in situ</i> )	$\Omega_{\text{arag}}$
Autumn	North Yellow Sea	13–16 Oct. 2017 <sup>b</sup>	16.6 ± 3.4	32.0 ± 0.1	89 ± 13%	2300 ± 10	2119 ± 54	0.921 ± 0.023	7.97 ± 0.09	2.16 ± 0.53
	South Yellow Sea	13, 18–27 Oct. 2017	17.5 ± 4.2	32.0 ± 0.3	92 ± 12%	2295 ± 21	2089 ± 70	0.910 ± 0.027	8.01 ± 0.10	2.41 ± 0.63
	northern ECS	31 Oct.–7 Nov. 2017	21.9 ± 1.1	33.6 ± 0.6	98 ± 3%	2242 ± 8	2001 ± 26	0.892 ± 0.011	8.02 ± 0.03	2.73 ± 0.23
Early winter	North Yellow Sea	30 Dec. 2017–8 Jan. 2018 <sup>b</sup>	7.8 ± 0.9	32.3 ± 0.1	97 ± 1%	2324 ± 11	2169 ± 14	0.933 ± 0.005	8.04 ± 0.03	1.81 ± 0.12
	South Yellow Sea	18–30 Dec. 2017	10.6 ± 1.2	32.3 ± 0.2	96 ± 6%	2320 ± 22	2146 ± 25	0.925 ± 0.011	8.04 ± 0.06	2.00 ± 0.24
	northern ECS	19–20 Dec. 2017	13.0 ± 0.9	32.8 ± 0.4	98 ± 1%	2283 ± 23	2101 ± 24	0.920 ± 0.003	8.03 ± 0.02	2.08 ± 0.07
Early spring	North Yellow Sea	8–16 Apr. 2018	4.8 ± 0.8	32.3 ± 0.3	107 ± 3%	2330 ± 23	2167 ± 25 <sup>c</sup>	0.930 ± 0.006 <sup>c</sup>	8.11 ± 0.04 <sup>c</sup>	1.85 ± 0.13 <sup>c</sup>
	South Yellow Sea	28 Mar.–8 Apr. 2018	7.2 ± 1.6	32.5 ± 0.4	105 ± 4%	2324 ± 26	2161 ± 33	0.930 ± 0.009	8.07 ± 0.05	1.87 ± 0.19
	northern ECS	1–2 Apr. 2018	9.6 ± 0.6	32.5 ± 0.6	104 ± 3%	2300 ± 16	2137 ± 24	0.930 ± 0.006	8.03 ± 0.02	1.85 ± 0.12
Late spring	North Yellow Sea	9–11 May 2018	7.6 ± 2.6	32.4 ± 0.1	104 ± 5%	2332 ± 17	2169 ± 28	0.930 ± 0.009	8.06 ± 0.03	1.89 ± 0.22
	South Yellow Sea	12–19 and 29–30 May 2018	11.7 ± 3.4	32.5 ± 0.4	102 ± 9%	2306 ± 22	2130 ± 43	0.924 ± 0.015	8.03 ± 0.07	2.02 ± 0.35
	northern ECS	23–28 May 2018	16.7 ± 3.0	32.3 ± 0.9	99 ± 14%	2261 ± 19	2053 ± 59	0.908 ± 0.022	8.03 ± 0.08	2.38 ± 0.51
Summer	North Yellow Sea	2–5 Aug. 2018	16.7 ± 8.4	31.9 ± 0.3	104 ± 10%	2318 ± 19	2127 ± 56	0.918 ± 0.019	7.99 ± 0.05	2.26 ± 0.53
	South Yellow Sea	24 Jul.–2 Aug. 2018	19.3 ± 7.3	31.8 ± 1.1	96 ± 19%	2296 ± 43	2104 ± 77	0.916 ± 0.025	7.96 ± 0.08	2.32 ± 0.65
	northern ECS	12–20 Jul. 2018	23.0 ± 2.9	32.2 ± 2.6	74 ± 29%	2234 ± 31	2042 ± 80	0.914 ± 0.033	7.90 ± 0.13	2.33 ± 0.81
Autumn	North Yellow Sea	24 Oct.–4 Nov. 2018	14.7 ± 2.3	31.9 ± 0.2	88 ± 12%	2307 ± 12	2143 ± 45	0.929 ± 0.017	7.96 ± 0.07	1.96 ± 0.40
	South Yellow Sea	14–24 Oct. 2018	17.7 ± 4.9	32.0 ± 0.5	89 ± 13%	2302 ± 25	2106 ± 74	0.915 ± 0.026	7.98 ± 0.08	2.32 ± 0.62
	northern ECS	8–14 Oct. 2018	23.8 ± 1.0	32.6 ± 1.6	91 ± 10%	2233 ± 18	2002 ± 32	0.896 ± 0.015	7.98 ± 0.04	2.69 ± 0.32

<sup>a</sup>Data were summarized by mean ± standard deviation across all stations and samples. TAlk, total alkalinity; DIC, dissolved inorganic carbon. <sup>b</sup>Some of the data collected from these surveys have been partially reported by Li (2019). <sup>c</sup>Calculated from field-measured TAlk and pH<sub>NBS</sub> data, since DIC samples collected during this survey were accidentally damaged before determination.

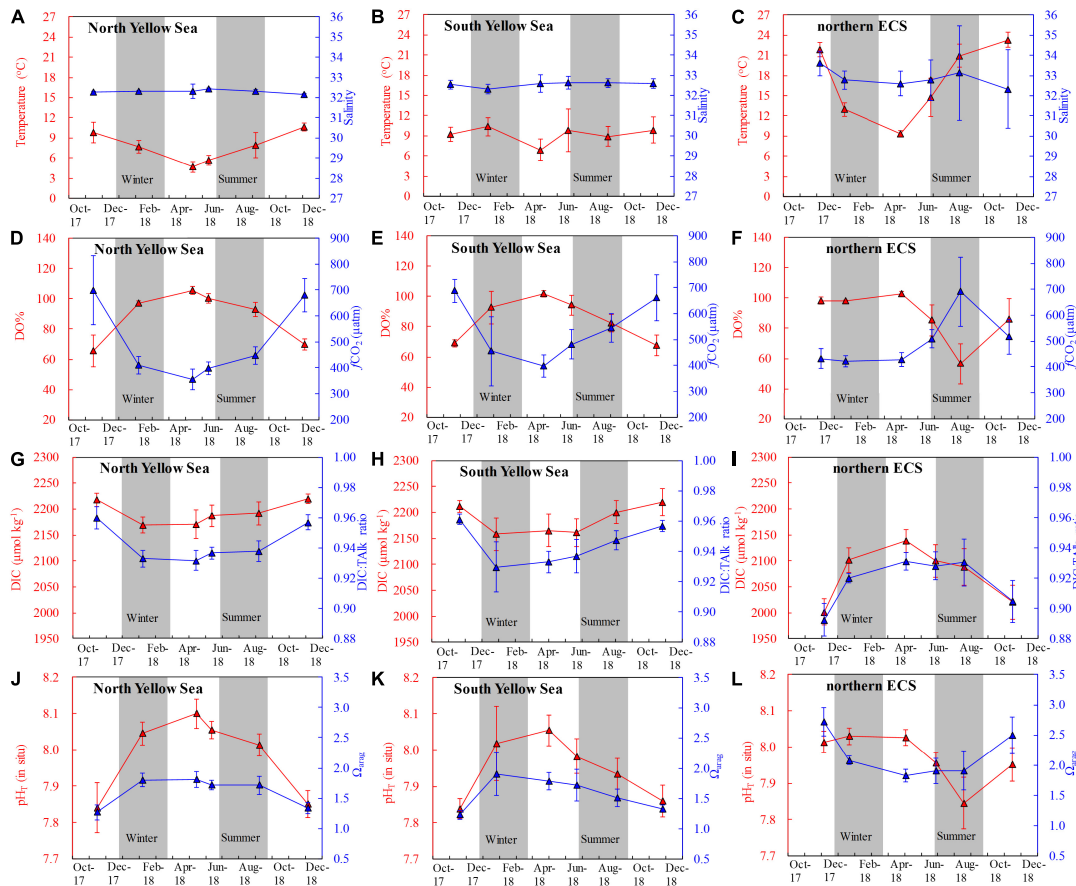


**FIGURE 2 |** Time series of survey-averaged values of bottom-water (A–C) temperature and salinity, (D–F) DO saturation (DO%) and fugacity of CO<sub>2</sub> (*f*CO<sub>2</sub>), (G–I) dissolved inorganic carbon (DIC) and DIC:TALK ratio, and (J–L) pH<sub>T</sub> (*in situ*) and aragonite saturation state ( $\Omega_{arag}$ ). TALK = Total alkalinity. Data points in the Yellow Sea during summer to autumn are within the YSCWM. Error bars denote standard deviations.

(~50 days), its bottom-water averaged apparent DO depletion rate (from 85% or 215  $\mu\text{mol O}_2 \text{ kg}^{-1}$  in late spring to 56% or 126  $\mu\text{mol O}_2 \text{ kg}^{-1}$  in summer) was estimated to be 1.8  $\mu\text{mol O}_2 \text{ kg}^{-1} \text{ d}^{-1}$ .

In addition, moderately low bottom-water DO values of ~140  $\mu\text{mol O}_2 \text{ kg}^{-1}$  were also observed in autumn at several southeastern stations (Figure 3F), where water temperature was moderately low (~22°C) (Supplementary Figure S6F), and salinity was quite high (~34) (Figure 1G), likely resulted from the TWWC that intruded into the northern ECS (Figure 1A).

### TALK

Survey-averaged TALK in the North Yellow Sea ranged between  $2300 \pm 10 \mu\text{mol kg}^{-1}$  and  $2332 \pm 17 \mu\text{mol kg}^{-1}$  (Table 1, with the annual mean of  $2316 \pm 19 \mu\text{mol kg}^{-1}$ ), while survey-averaged TALK in the South Yellow Sea ranged between  $2295 \pm 21 \mu\text{mol kg}^{-1}$  and  $2324 \pm 26 \mu\text{mol kg}^{-1}$  (Table 1, with the annual mean of  $2305 \pm 31 \mu\text{mol kg}^{-1}$ ). In the northern ECS, however, relatively low TALK values were observed, ranging from  $2233 \pm 18 \mu\text{mol kg}^{-1}$  to  $2300 \pm 16 \mu\text{mol kg}^{-1}$  (Table 1, with the annual mean of  $2243 \pm 28 \mu\text{mol kg}^{-1}$ ).

Talk versus salinity showed different relationships in the three regions (Figures 4A–C). In the North Yellow Sea, TALK versus salinity roughly followed Eq. (1), although TALK data obtained from our five cruises in 2018 were 10–30  $\mu\text{mol kg}^{-1}$  higher than those values predicted by salinity and Eq. (1). In the South Yellow Sea, however, quite complicated water mixing behaviors were involved (Figure 4B). In the northern ECS, many data points of TALK versus salinity fairly followed a linear relationship (Figure 4C), i.e.,

$$\text{TALK}^{\text{northern\_ECS}} = 11.922 \times \text{Salinity} + 1850 (R^2 = 0.94, n = 172) \quad (2)$$

Equation (2) indicated a two-endmember water mixing between the Changjiang freshwater ( $S = 0$ , TALK = 1850  $\mu\text{mol kg}^{-1}$ ) and the ECS offshore waters ( $S = 34.9$ , TALK = 2266  $\mu\text{mol kg}^{-1}$ ), as derived from our July 2018 cruise conducted off the Changjiang Estuary (Figure 1). This linear relationship also roughly characterized several ECS nearshore stations (along the China's east coast) sampled during

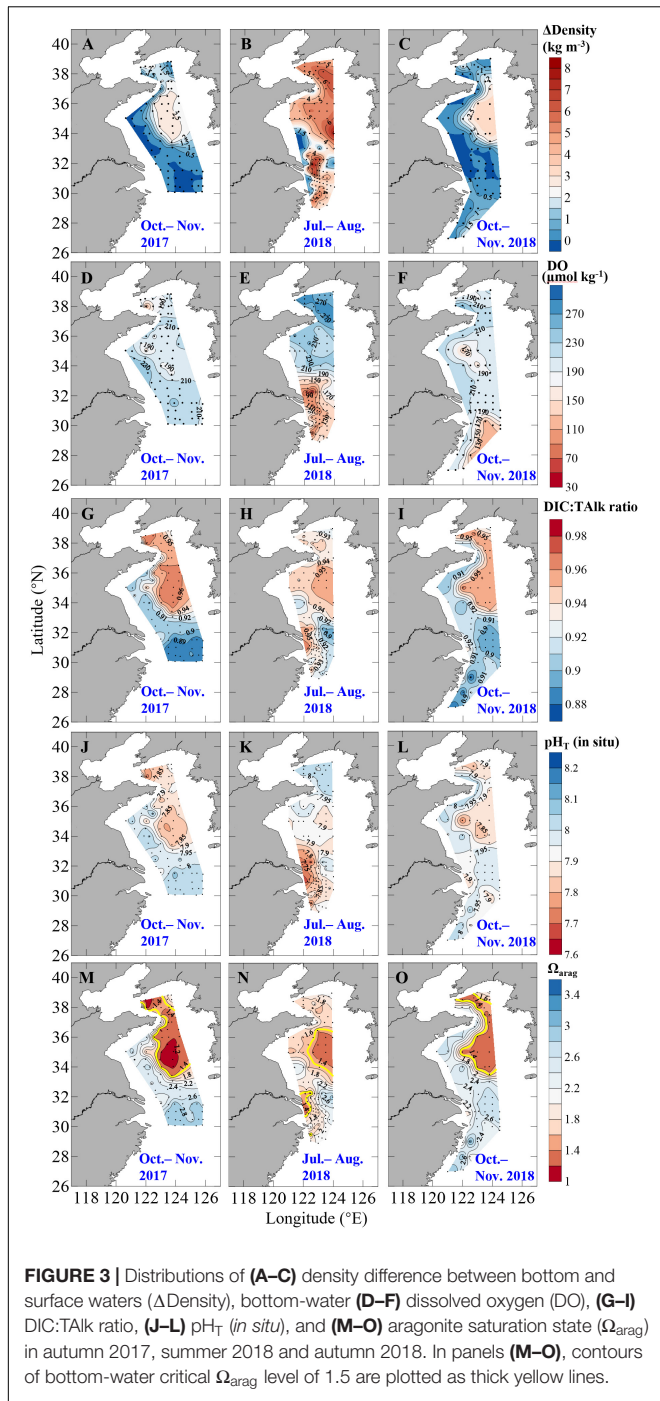


**FIGURE 3 |** Distributions of (A–C) density difference between bottom and surface waters ( $\Delta$ Density), bottom-water (D–F) dissolved oxygen (DO), (G–I) DIC:TALK ratio, (J–L)  $\text{pH}_T$  (*in situ*), and (M–O) aragonite saturation state ( $\Omega_{\text{arag}}$ ) in autumn 2017, summer 2018 and autumn 2018. In panels (M–O), contours of bottom-water critical  $\Omega_{\text{arag}}$  level of 1.5 are plotted as thick yellow lines.

our autumn 2018 cruise, with quite low salinity values of 26.0–30.5 (Figure 1G) and TALK values of 2138–2229  $\mu\text{mol kg}^{-1}$  (Figure 4C), indicating that the southward-moving ZFCC was closely coupled with the CDW (Figure 1A). In winter and spring, however, quite high TALK values of 2283–2333  $\mu\text{mol kg}^{-1}$  at moderate salinity values of 31.3–32.8 were observed in the northern ECS (Figure 4C), showing the intrusion of the northeast monsoon-driven YSCC (Figure 1A).

## DIC and DIC:TALK Ratio

The Yellow Sea exhibited higher DIC values than the northern ECS (Figures 2G,H versus Figure 2I). Annual mean DIC values were  $2145 \pm 47 \mu\text{mol kg}^{-1}$  in the North Yellow Sea,  $2119 \pm 65 \mu\text{mol kg}^{-1}$  in the South Yellow Sea, and  $2031 \pm 65 \mu\text{mol kg}^{-1}$  in the northern ECS. Wintertime and springtime DIC values in the North Yellow Sea were averaged at  $2168 \pm 22 \mu\text{mol kg}^{-1}$  (Figure 4D), while wintertime and springtime DIC values in the South Yellow Sea were averaged at  $2144 \pm 36 \mu\text{mol kg}^{-1}$  (Figure 4E). In the Yellow Sea, DIC data showed greater vertical variations in summer and autumn than in winter and spring (Supplementary Figures S3–S5), and the YSCWM had relatively high DIC values of 2150–2270  $\mu\text{mol kg}^{-1}$  in summer and autumn (Figures 4D,E). In the northern ECS, the low DIC values of this study of 1650–1950  $\mu\text{mol kg}^{-1}$  were observed in the summertime ECS surface waters (Supplementary Figure S7F), while the ECS bottom-water DIC values were mostly 2050–2150  $\mu\text{mol kg}^{-1}$  in summer (Figure 4F).

The Yellow Sea usually had higher DIC:TALK ratios than the northern ECS (Figures 2G–I). From early winter to late spring, survey-averaged DIC:TALK ratio in the North Yellow Sea ranged between  $0.930 \pm 0.009$  and  $0.933 \pm 0.005$  (Table 1), usually at  $0.930 \pm 0.010$  (Figure 4G), while survey-averaged DIC:TALK ratio in the South Yellow Sea varied from  $0.924 \pm 0.016$  to  $0.930 \pm 0.009$  (Table 1), usually at  $0.925 \pm 0.010$  (Figure 4H). In the YSCWM (with salinity of  $> 32$  and temperature of  $< 12^\circ\text{C}$ ), bottom-water DIC:TALK ratios increased to  $0.944 \pm 0.008$  in summer and  $0.959 \pm 0.005$  in autumn (Figures 3G–I, 4G,H). In early winter, several very high bottom-water DIC:TALK ratio values of 0.958–0.967 (Figure 4H) were observed at the four deep stations in the central South Yellow Sea, together with DO% of 65–72% and  $f\text{CO}_2$  of 672–806  $\mu\text{atm}$  (Supplementary Figure S5).

In the northern ECS, survey-averaged DIC:TALK ratio values in early winter ( $0.920 \pm 0.003$ ) and early spring ( $0.930 \pm 0.006$ ) were much higher than the usual ratio of  $\sim 0.9$  in the ECS offshore waters (Table 1), but quite close to the usual DIC:TALK ratio of wintertime and springtime Yellow Sea waters (Figures 2G–I). This was likely because the YSCC transported the Yellow Sea waters into the northern ECS during the northeast monsoon season (Figure 1A). In late spring, the ECS DIC:TALK ratio tended to show limited vertical gradient, with surface values of  $0.891 \pm 0.013$  (Supplementary Figure S7I) and bottom-water values of  $0.928 \pm 0.009$  (Figure 4I). In general, the ECS bottom waters increased their DIC:TALK ratio values to 0.930–0.970 in summer, and then declined to  $< 0.9$  in autumn (Figures 3G–I). At several nearshore stations affected by the ZFCC and those southeastern stations likely affected by the TWWC intrusion, relatively high bottom-water DIC:TALK ratio values of 0.920–0.930 were also revealed during our autumn 2018 cruise (Figures 3I, 4I).

## Bottom-Water AOU and Excess DIC From Late Spring to Autumn

In late spring, both bottom-water AOU and ExcessDIC varied around 0 in the North Yellow Sea (Figure 5A), while the South Yellow Sea bottom-water AOU and ExcessDIC

Download of the whole book:

<https://www.frontiersin.org/research-topics/12104/acidification-and-hypoxia-in-marginal-seas>